

A Regional Approach to M/EEG Source Estimation: Characterizing the Tradeoff between Spatial Resolution and Signal Discriminability

M.E. Pflieger & R.E. Greenblatt
Source Signal Imaging, Inc.
<http://www.sourcesignal.com>

NeuroImage 13(6):S219 (abstract)

Poster presented at HBM 2001 (7th Annual Meeting of the Organization of Human Brain Mapping), Brighton, UK, 10-14 June 2001. *Updated 6/26/2001 with results obtained via an improved estimator.*

<http://www.academicpress.com/www/journal/hbm2001/11433.html>

Correspondence:

Mark E. Pflieger

2323 Broadway, Suite 102

San Diego, CA 92102 USA

email: mep@sourcesignal.com

phone: +1-619-234-9935 ext 15

Introduction

Except for the special case of singly active sources, characterization of the 3D spatial resolution of magneto- and electro-encephalography (M/EEG) remains an open issue. The underlying difficulty arises from the circumstance that most source estimators aim to solve a global inverse problem, that is, to find a complete solution in the brain that can account for all measured data at the outer head surface (typically with regularization). Whether the underlying source model is discrete and overdetermined (e.g., several dipoles) or distributed and underdetermined (e.g., cortically constrained current density), all global estimators yield source estimates that are linearly coupled across locations. Consequently, an estimation error at one location propagates errors to other locations in a complex network, which renders spatial resolution difficult to characterize in general. Local source estimators, on the other hand, do not attempt to solve the global inverse problem. Rather, they solve for linear transformations of the measurements that optimize, in some sense, estimates of source activity at a given location, independently of estimates at other locations. A linearly constrained minimum variance beamformer ([1], [2], [3]) is an example of an underdetermined local estimator, whereas optimally localized averaging (OLA) of both multiplicative (MOLA, or Backus-Gilbert method [4]) and subtractive (SOLA [5]) varieties are overdetermined local estimators.

REGAE

We describe a new **regional** approach to local source estimation, called REGAE (regional activity estimation), which has SOLA as its nearest relative. SOLA optimizes a tradeoff between two parameters (spatial resolution and noise sensitivity), whereas REGAE, specialized for probabilistic regions centered on a point (pREGAE), optimizes a tradeoff between three parameters (false alarm rate, hit rate, and spatial resolution) within the framework of signal detection theory. Specification of a threshold converts an estimator into a detector. False alarm rate is the probability of falsely detecting a source signal from a region of interest (ROI) when the measured activity actually has no ROI component. Hit rate is the probability of correctly detecting ROI signals in the presence non-ROI signals and other noise. Jointly, false alarm rate and hit rate determine a detector's **discriminability**, indexed by d' , which is the area under the **receiver operator characteristic** (ROC) curve. In the case of pREGAE, the ROI has a 3D gaussian probability density centered on a point of interest. Signal discriminability increases as the spatial spread of this distribution increases. Thus, there is an inherent tradeoff between spatial resolution and signal discriminability, which pREGAE attempts to optimize. Using realistic head and source space models, we characterize this theoretical tradeoff as a function of EEG sensor density (32 to 256 channels) and source location (parietal, temporal pole, and anterior cingulate cortices).

Regional Activity Estimation & Detection

An **estimator** of regional source activity is a function f , which has the general form

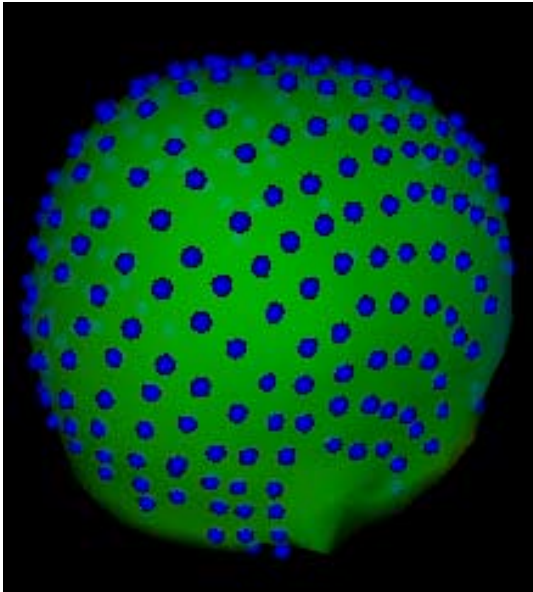
$$\hat{\alpha} = f[\mathbf{S}_{sp}, \mathbf{S}_{sig}, \mathbf{R}, \mathbf{M}_{cfg}, \mathbf{M}_{snr}, \mathbf{H}](\mathbf{v})$$

where

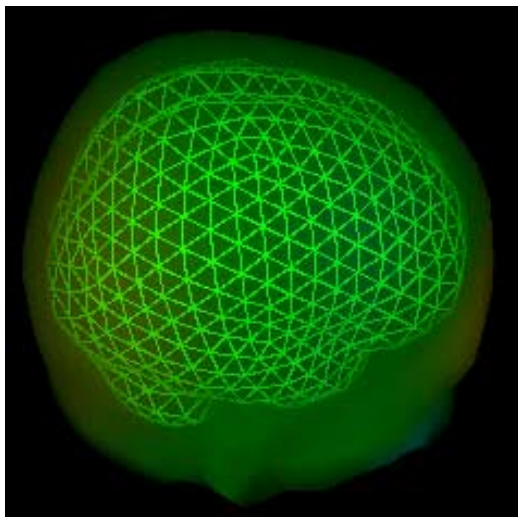
- $\hat{\alpha}$ Estimated total activity in a region of interest
- \mathbf{S}_{sp} Source space model = locations and orientations of current dipole elements
- \mathbf{S}_{sig} A priori model of signal statistics in the source space
- \mathbf{R} Region of Interest (ROI) = source space vector with values in [0,1]
- \mathbf{M}_{cfg} Geometric configuration of sensors, which determines a measurement space
- \mathbf{M}_{snr} Statistical models of signal & noise in the measurement space
- \mathbf{H} Head model of volume conduction from source signals to measured signals
- \mathbf{v} Measurement vector

Given an estimator, a **detector** of activity in a ROI is determined by specifying a threshold, θ , such that ROI activity is judged to be present if and only if $\hat{\alpha} > \theta$. Detection performance is characterized by varying the threshold to generate a ROC (receiver operator characteristic) curve of hit rate (1.0 – Type II error probability) as a function of false alarm rate (Type I error probability). *REGAE assesses estimation quality via signal detection performance.*

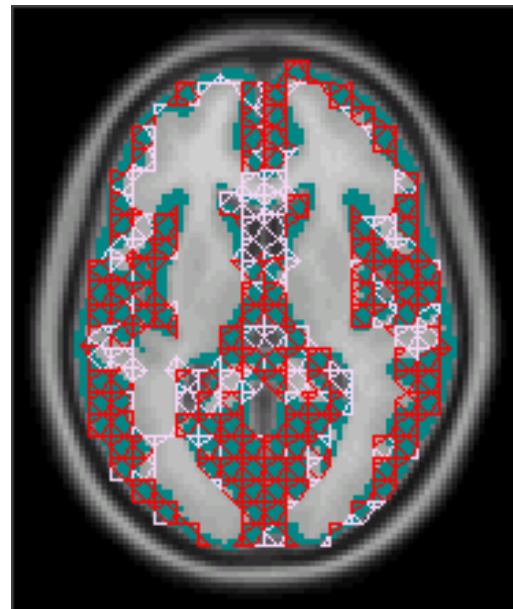
Specific assumptions made in this study



256 Electrode Configuration



BEM Head Model
(Scalp & Inner Skull shown)



Source Space model:
Tetrahedral mesh of a
gray matter segmentation
of the MNI average brain
(3152 locations, 3 dipoles
per location)

Source signal statistics were assumed to be gaussian and i.i.d. throughout the source space.

Regions of interest were defined as 3D gaussian distributions centered on points of interest.

The total signal subspace of measurement space was unrestricted, and instrumental noise was assumed to be zero.

Based on the principles of regional projection and maximum ROI/non-ROI discriminability, the REGAE estimator determines a matrix \mathbf{E} , in a manner to be described elsewhere, such that $\hat{\alpha} = \sqrt{\mathbf{v}^T \mathbf{E}^T \mathbf{E} \mathbf{v}}$.

Results

ROIs: Figures 1(a), 2(a), and 3(a) show concentric ROIs centered on points of interest in parietal, anterior cingulate, and temporal pole cortices, respectively. Each ROI is restricted to a gray matter segmentation of the MNI average brain. Shown are the full-width at half-maximum (FWHM) diameters for gaussian spreads about the points of interest.

ROC curves: 256-channel receiver operator characteristic (ROC) curves for the three regions, for various spatial spreads, are shown in figures 1(b), 2(b), and 3(b). Hit rates were obtained by simulating independent and identically distributed activity throughout the source space, including the ROI, whereas false alarm rates were obtained by simulating non-ROI activity only. These curves illustrate the inverse relationship between signal discriminability and spatial resolution. For example, in the parietal region using 256 EEG channels, if the probability of a Type I error (false positive) is fixed at 0.05, then Type II error (miss) probabilities of 0.70, 0.30, 0.10, and 0.03 can be achieved via spatial spreads (FWHM) of 20 mm, 30 mm, 40 mm, and 50 mm, respectively.

Discriminability/Resolution curves: In figures 1(c), 2(c), and 3(c), ROI/non-ROI discriminability (d' = area under the ROC curve) is plotted as a function of spatial spread of the ROI (= 1/resolution) for 32, 64, 128, and 256 channel configurations. The resulting curves are S-shaped (clipped on the right), with different characteristics for different regions. Of the three regions, the parietal performance was best. For each doubling of the number of channels, there is a significant improvement of discriminability/resolution, which continues up to 256 channels.

Parietal ROIs

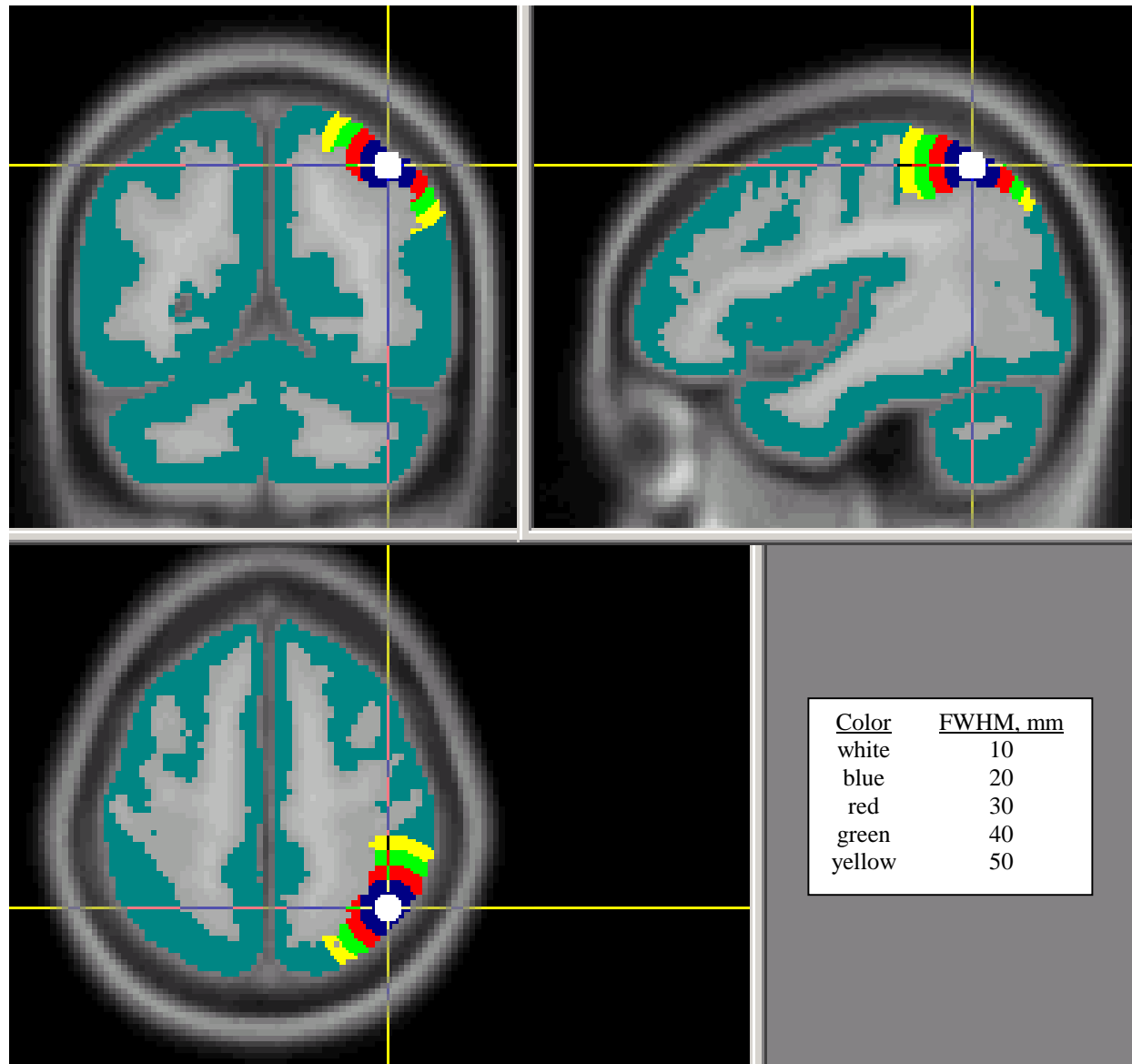


Fig. 1(a)

Parietal Region ROC Curves

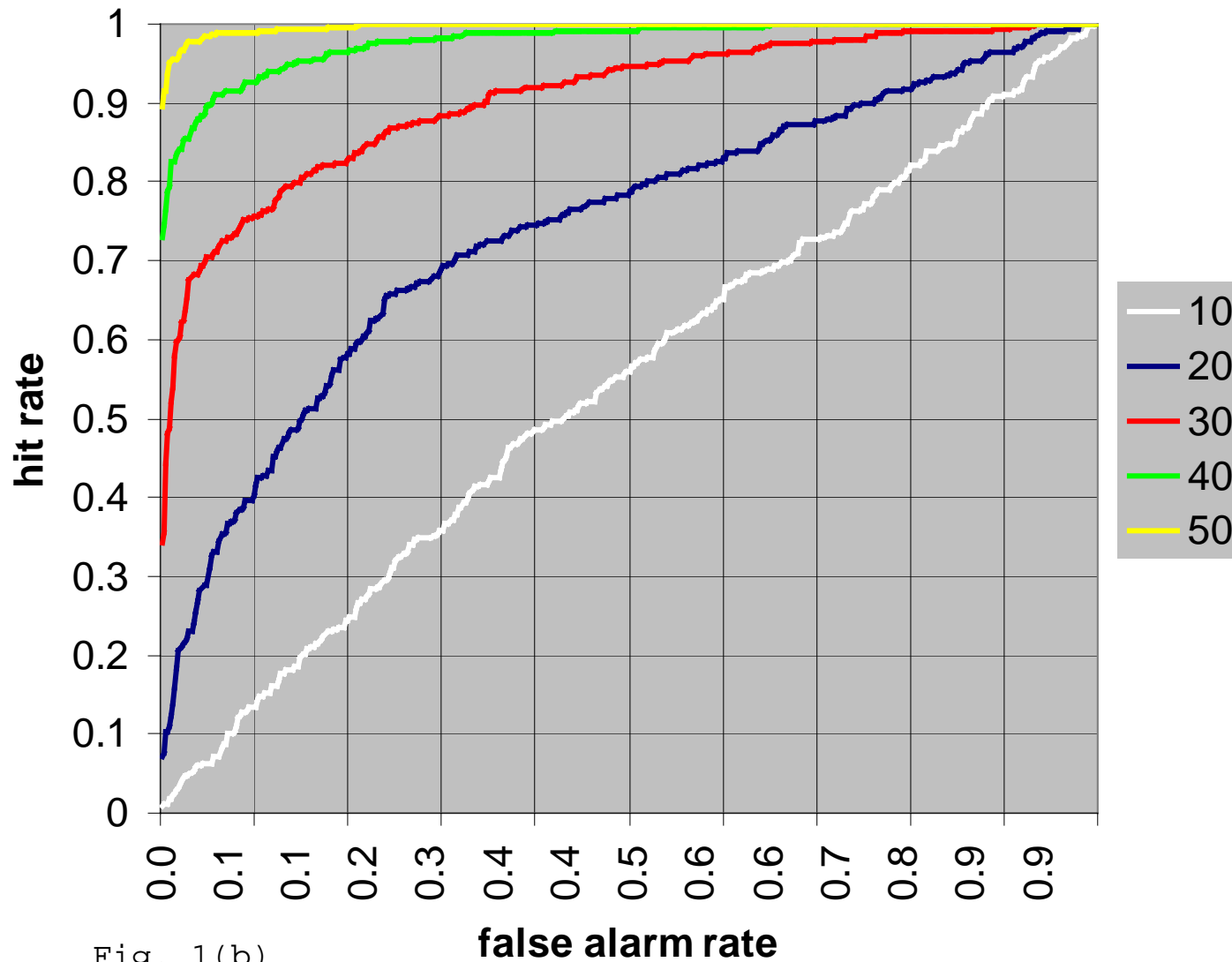


Fig. 1(b)

256 Channels, Various Spreads (FWHM, mm)

Parietal Discriminability/Resolution Curves

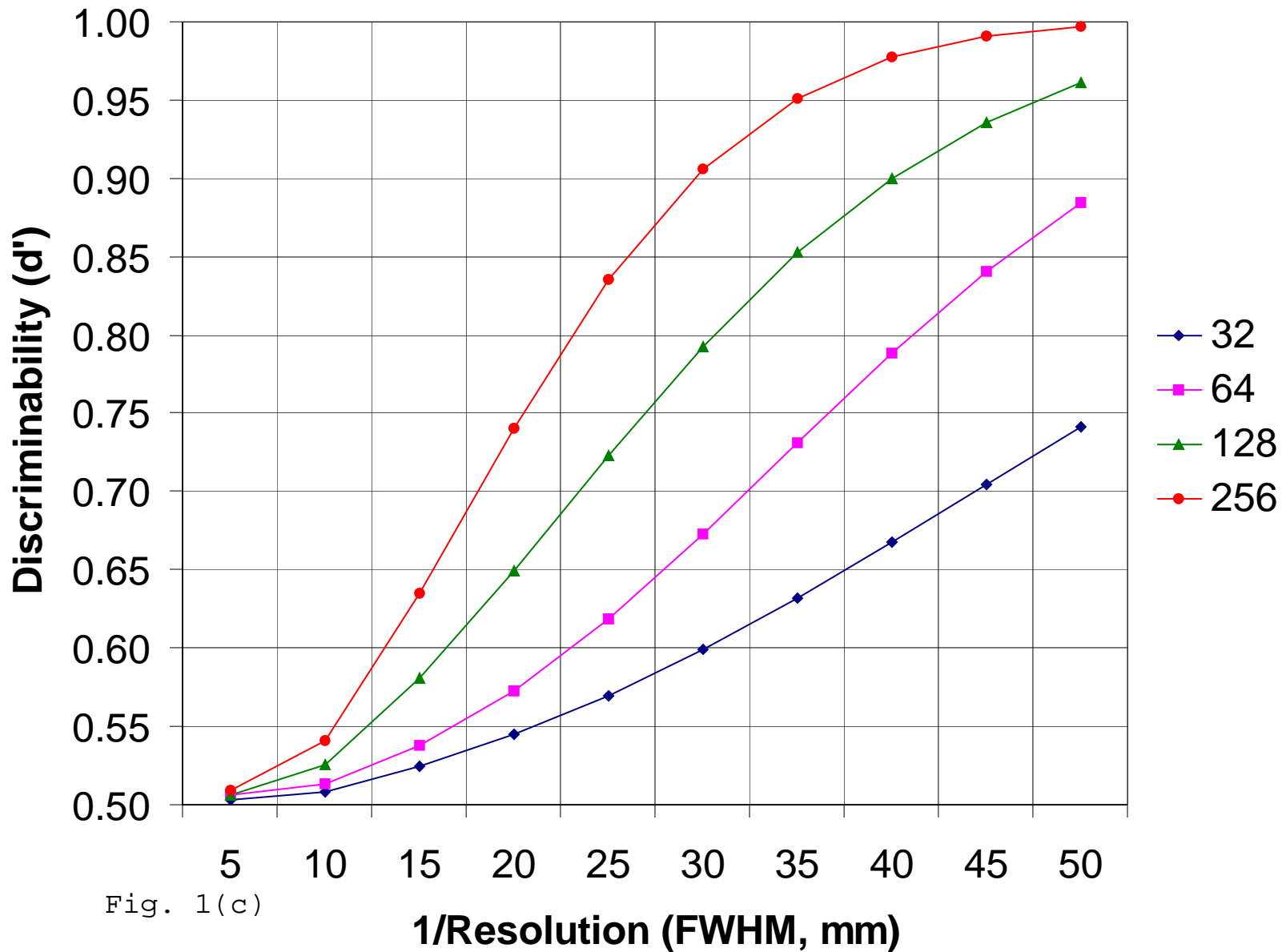


Fig. 1(c)

Bilateral Anterior Cingulate ROIs

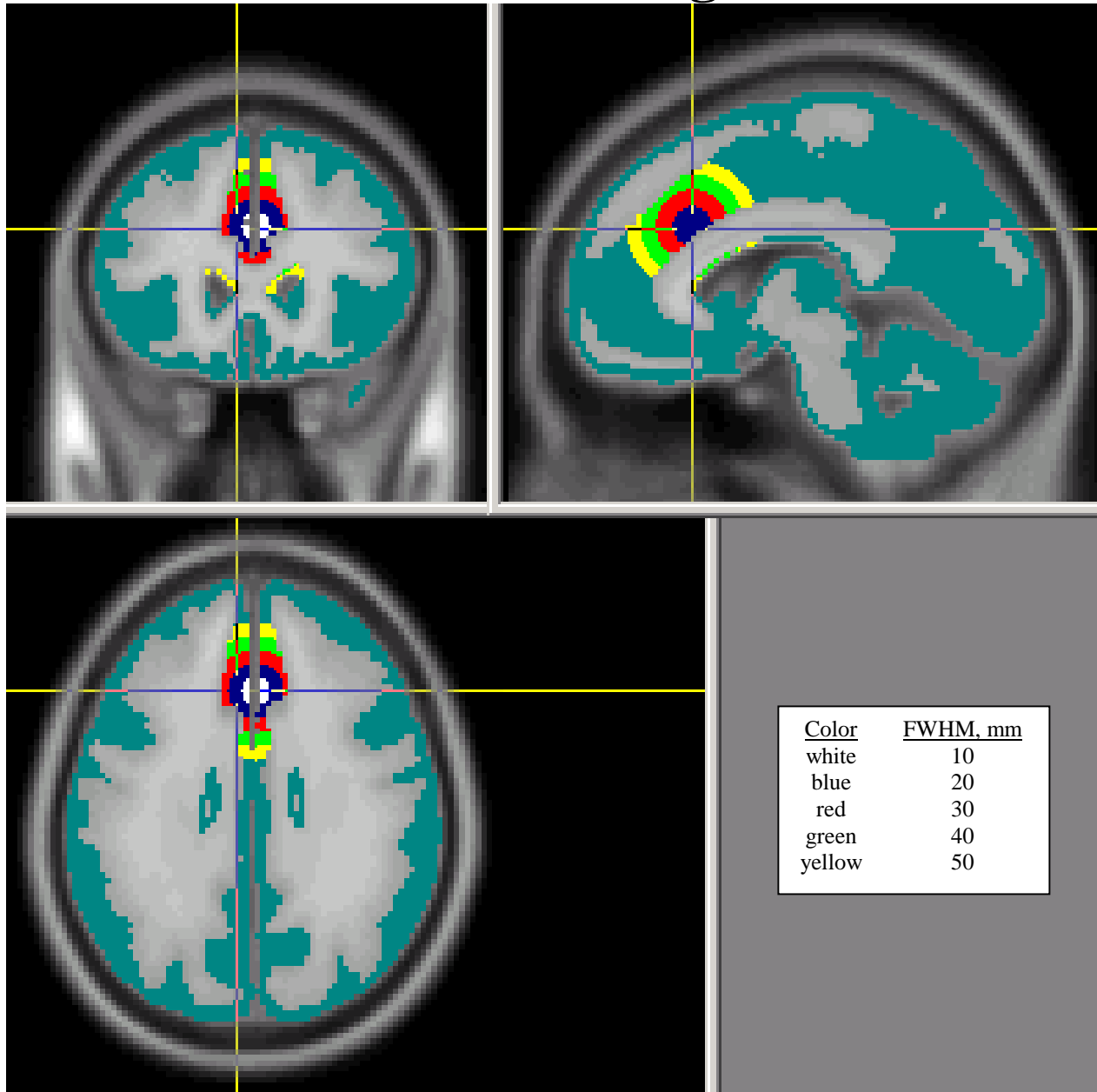


Fig. 2(a)

Anterior Cingulate Region ROC Curves

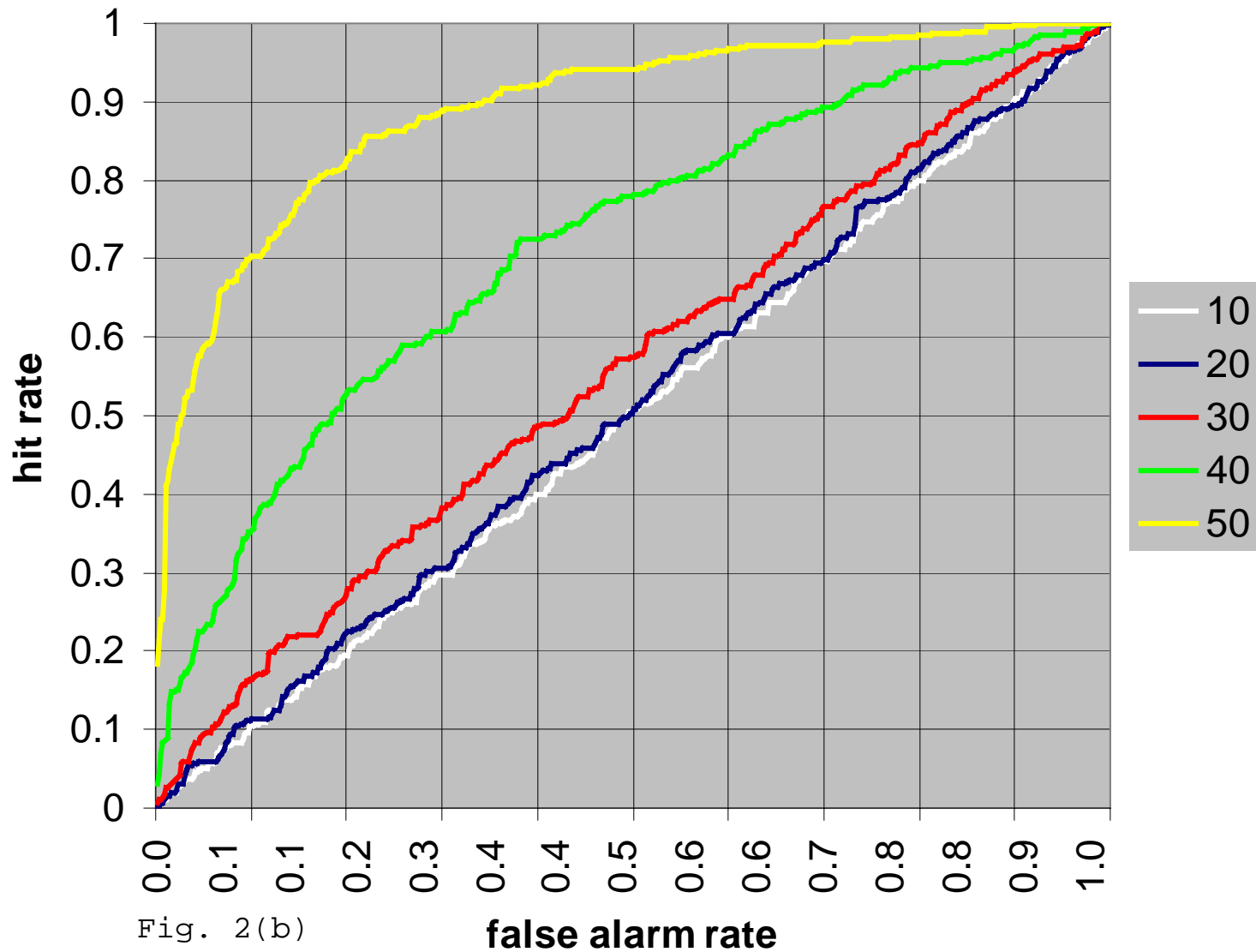


Fig. 2(b)

256 Channels, Various Spreads (FWHM, mm)

Anterior Cingulate Discriminability/Resolution Curves

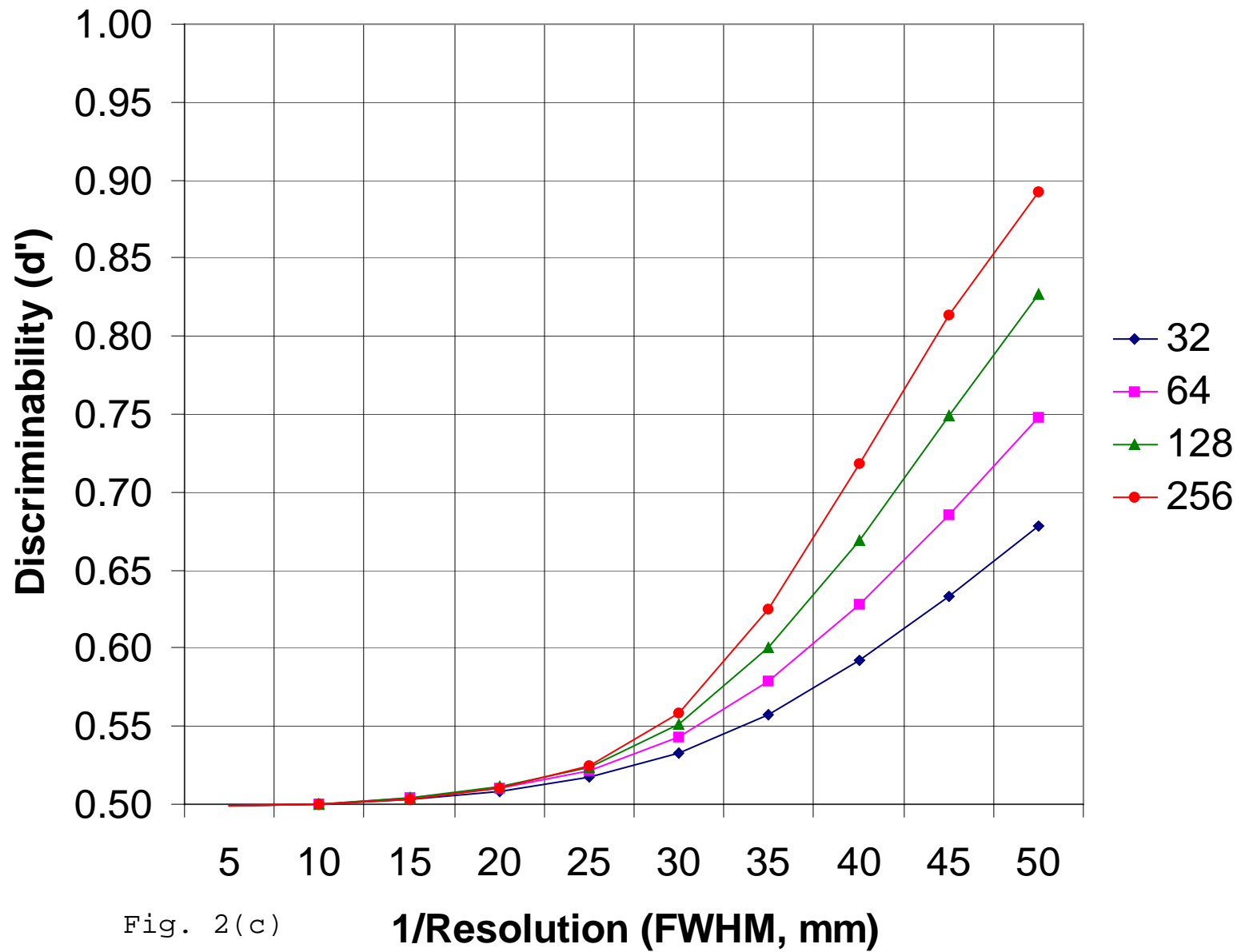


Fig. 2(c)

Temporal Pole ROIs

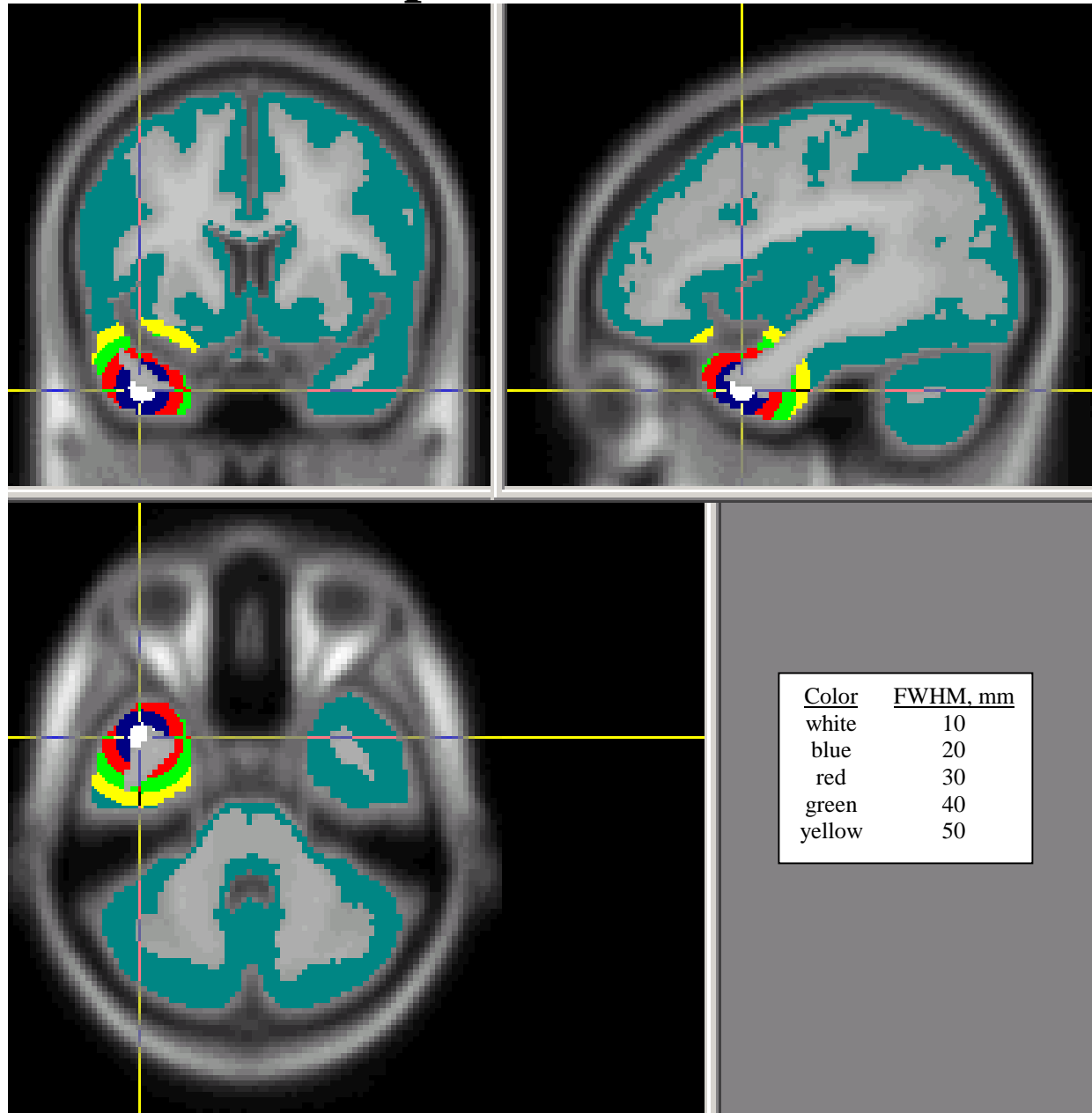


Fig. 3(a)

Temporal Pole Region ROC Curves

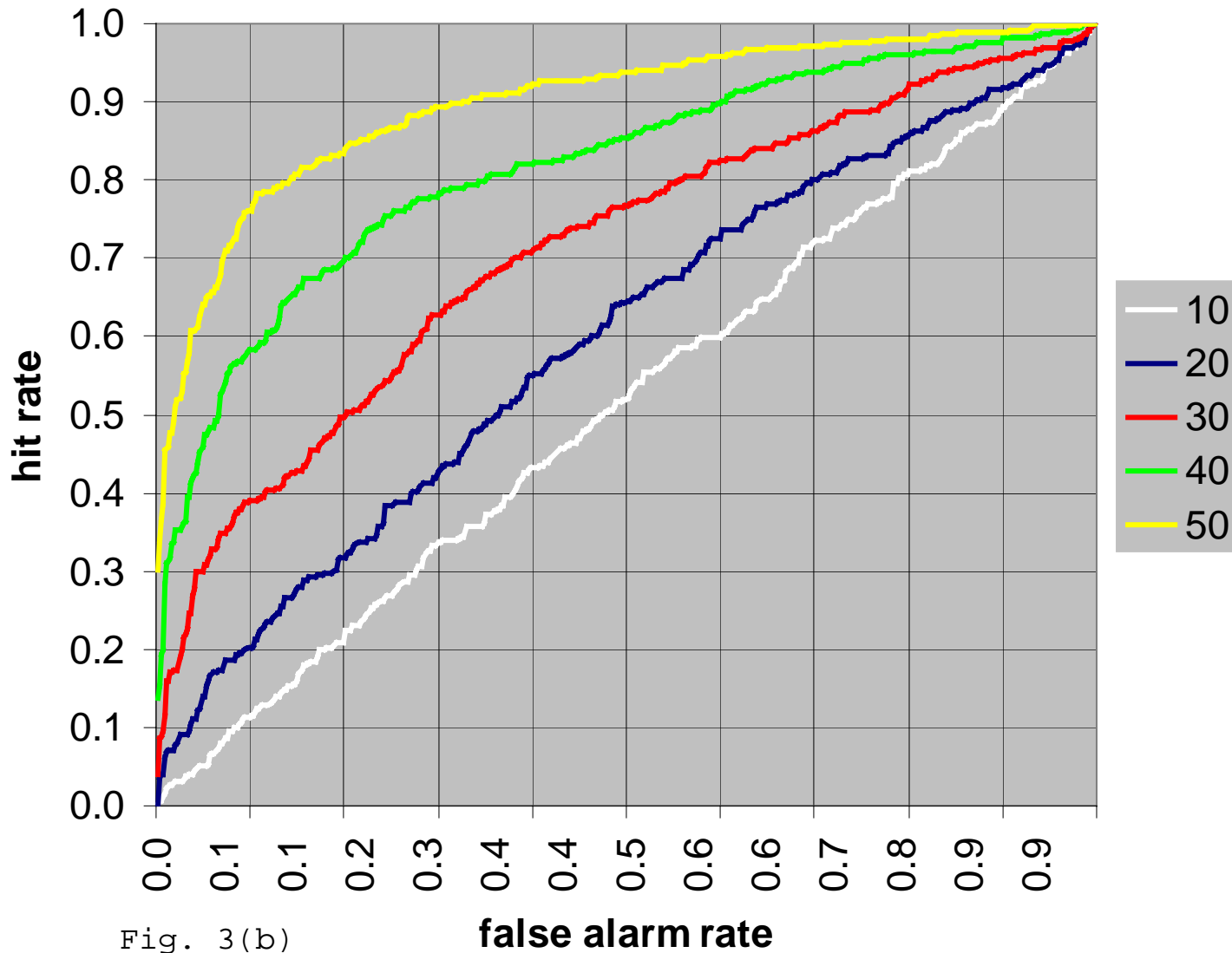


Fig. 3(b)

256 Channels, Various Spreads (FWHM, mm)

Temporal Pole Discriminability/Resolution Curves

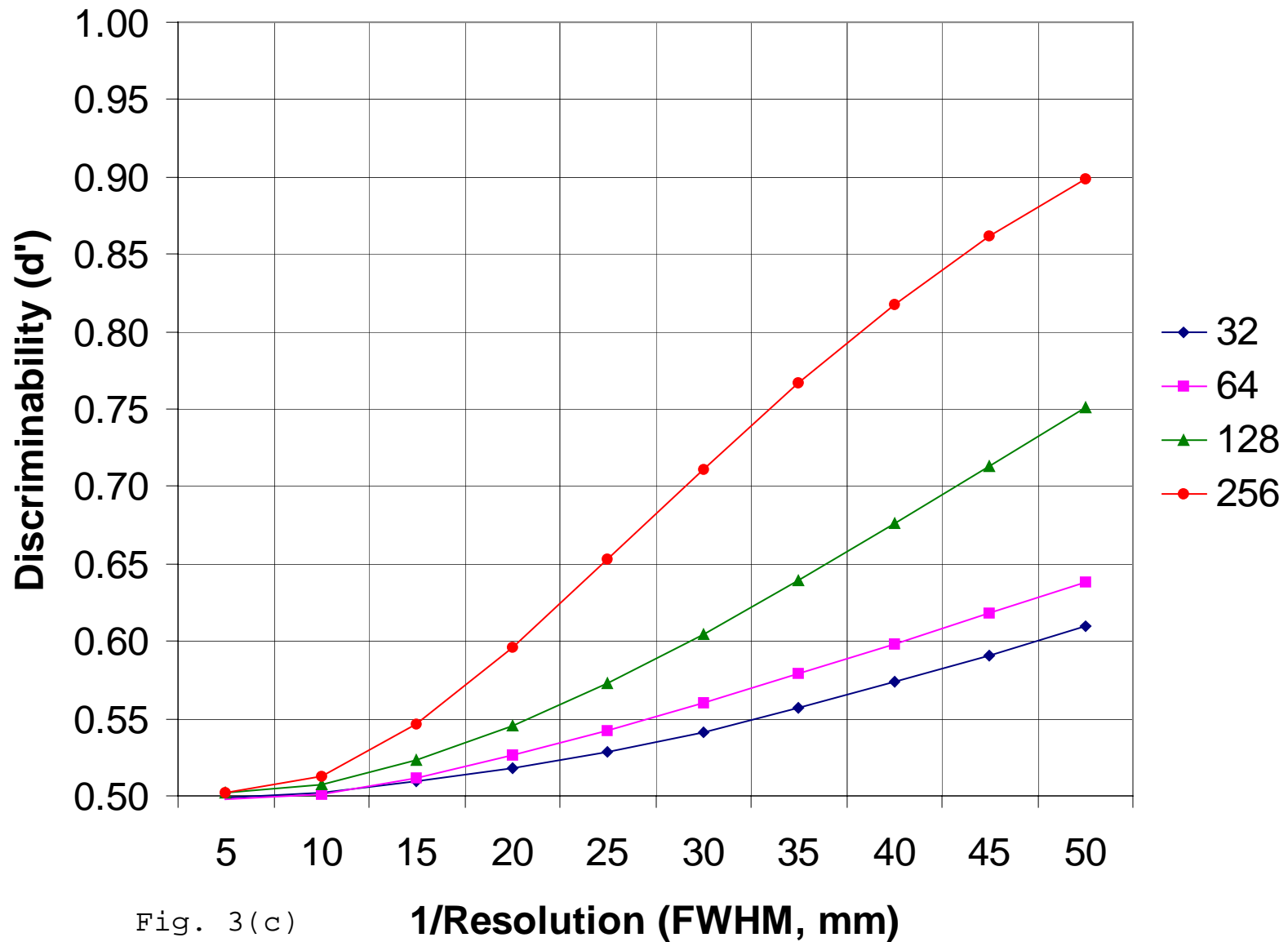


Fig. 3(c)

Discussion

References [6], [7], and [8] illustrate the difficulty of characterizing the 3D spatial resolution of M/EEG when more than one or two point sources are simultaneously active. Here we have introduced a new framework for source estimation, called REGAE, which provides an alternative approach to this problem. Since any or all locations within the brain's source space might contribute to the measured activity, the problem is to distinguish "source states" that have a ROI contribution from those that do not. Thus, there is an inherent tradeoff between spatial resolution (the reciprocal of ROI size) and discriminability of ROI versus non-ROI signal. Here we have assumed a maximum entropy distribution of the source states, that is, equal and independent probabilities of activity across all locations in the source space. Because we have assumed in this study that everything of brain origin is signal of interest, the present analysis is particularly applicable to the estimation of ongoing brain activity.

Based on the three regions considered, it is apparent that signal discriminability and spatial resolution can vary considerably as a function of location of interest in the source space, with better performance for superficial cortex in the upper hemisphere of the head (where most of the sensors are located). At the same time, these "calibration curves" permit the equalization of different points of interest with respect to signal discriminability by varying ROI size.

The curves obtained here for EEG represent currently attainable discriminability and resolution, but not necessarily absolute limits. We expect to improve performance by using cortical surface source spaces for individual subjects, and by extending the analysis from ongoing activity to event-related activity via signal/noise models for specific tasks.

Literature Cited

- [1] Van Veen BD, van Drongelen W, Yuchtman M, Suzuki A (1997): Localization of brain electrical activity via linearly constrained minimum variance spatial filtering. *IEEE Trans Biomed Eng* 44:867-880.
- [2] Robinson SE, Vrba J (1999): Functional neuroimaging by synthetic aperture magnetometry (SAM). In: T Yoshimoto et al. (eds.), *Recent Advances in Biomagnetism*, Tohoku University Press, pp. 302-305.
- [3] Sekihara K, Nagarajan S, Poeppel D, Miyashita Y (2000): Reconstructing spatio-temporal activities of neural sources using MEG vector beamformer. *NeuroImage* 11(5):S485.
- [4] Press WH et al. (1992), *Numerical Recipes in C*, Cambridge, pp. 815-818, give a concise summary of the Backus-Gilbert theory.
- [5] Pijpers FP, Thompson FJ (1994): The SOLA method for helioseismic inversion. *Astron Astrophys* 281:231-240.
- [6] Mosher JC, Spencer ME, Leahy RM, Lewis PS (1993): Error bounds for EEG and MEG dipole source localization. *Electroencephalogr clin Neurophysiol* 86:303-321.
- [7] Pflieger ME (1998): Local maxima in EEG tomographies and their relation to multiple point sources. *Proc IEEE/EMBS* 20:2139-2142.
- [8] Pflieger ME, Nakada T (2000): The spatial resolving power of high-density EEG: an assessment of limits. In: T Nakada (Ed.), *Integrated Human Brain Science: Theory, Method, Application (Music)*, Elsevier Science. pp. 147-191.

Acknowledgements

We appreciate the assistance of Shugo Suwazono, who provided 3D locations for the Neuroscan ESI-256 electrode configuration, and of David Nichols, who enabled visualization of concentric ROIs. We gratefully acknowledge funding, in part, by grants from the NINDS and the NIMH.